Fermilab FERMILAB-Conf-00/111-E D0/CDF/E706 June 2000

QCD MEASUREMENTS AT THE TEVATRON

Cecilia E. Gerber
(for the DØ, CDF and E706 Collaborations)
Fermi National Accelerator Laboratory, P. O. Box 500, Batavia, IL 60510–500

Abstract

We present a review of recent QCD related results from the Fermilab Tevatron fixed target and collider experiments. Topics include studies of jet and photon production, and intermediate vector boson production and decay.

1 Introduction

Quantum Chromodynamics (QCD) emerged as a mathematically consistent theory in the 1970s, and nowadays is regarded as one of the cornerstones of the Standard Model. One of the triumphs of modern particle physics has been the extent to which QCD has successfully accounted for the strong interaction processes observed experimentally at hadron colliders. Some of the processes studied include hadronic jet, heavy quark, and gauge boson production.

The number of new results from the Fermilab Tevatron accelerator that are being presented at this conference is impressive. The two collider detectors, CDF and DØ, have finished taking data in 1996; new results on Jet and Boson properties are based on these large data sets of ~ 100 pb^{-1} integrated luminosity. Both collaborations are upgrading their detectors in preparation for Run II, scheduled to start in the year 2001. Photon production results from the fixed target experiment E706 are based on data taken during its last fixed target run that ended in 1992.

2 Jet Production in proton–antiproton collisions

At the Tevatron energies, the dominant process in $p\overline{p}$ collisions is jet production. Within the framework of QCD, inelastic scattering between a proton and an antiproton can be described as an elastic collision between a single proton constituent and a single antiproton constituent. These constituents are called partons. After the collision, the outgoing partons manifest themselves as localized streams of particles referred to as "jets". Theoretical predictions for jet production are given by the folding of the parton scattering cross sections with experimentally determined parton density functions (pdf's). These predictions have recently improved with next–to–leading order (NLO) QCD scattering calculations [1, 2, 3] and new, accurately measured pdf's [4, 5]. Some of the questions that can be addressed with studies of jet production are testing of NLO QCD, extraction of pdf's, measuring the value of the strong coupling constant α_s, and testing quark compositeness. In this writeup we present measurements of jet cross sections at center of mass energies of 1800 and 630 GeV, and of subjet multiplicities in quark and gluon jets.

2.1 Inclusive Jet Cross Section

The DØ and CDF collaborations measure the central inclusive jet cross section in $p\overline{p}$ collisions at $\sqrt{s} = 1.8$ TeV using an integrated luminosity of 92 pb^{-1} and 87 pb^{-1},

respectively. The inclusive double differential jet cross section can be expressed as:

$$d^2\sigma/(dE_T d\eta) = (N_{Jet})/(\varepsilon \Delta E_T \Delta\eta \int Ldt)$$

where N_{Jet} is the total number of jets observed in a certain jet transverse energy E_T bin, ε is the selection efficiency, ΔE_T is the bin width, $\Delta\eta$ is the pseudorapidity range considered, and $\int Ldt$ is the integrated luminosity associated with the data set. The cross sections are measured in the pseudorapidity interval $0.1 < |\eta| < 0.7$ (CDF), and the two pseudorapidity ranges $|\eta| < 0.5$ and $0.1 < |\eta| < 0.7$ (DØ [6]). Figure 1 shows the ratio plot (Data-Theory)/Theory for the $0.1 < |\eta| < 0.7$ rapidity range for CDF and DØ data compared to NLO QCD.

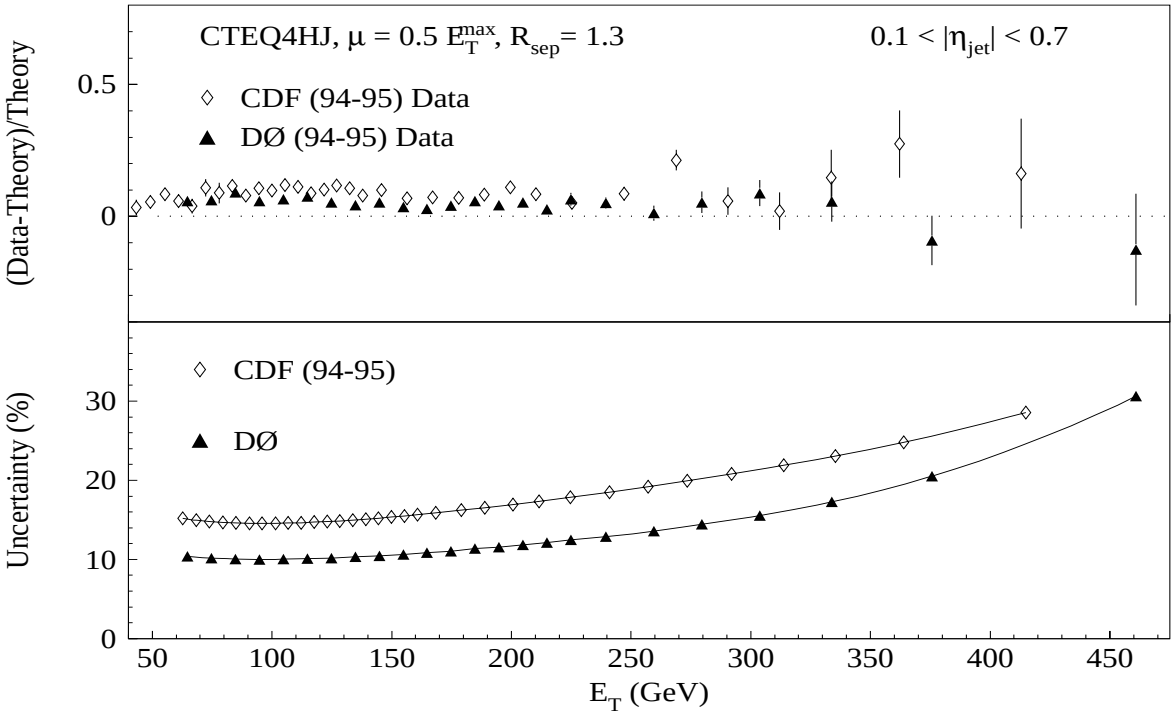

Figure 1: Inclusive jet cross section in the central rapidity region for CDF and DØ, plotted versus jet E_T. The data points are shown with statistical uncertainties. The systematic uncertainty on the ratio is shown in the bottom half of the plot.

In addition, DØ presented for the first time the preliminary measurement of the rapidity dependence of the inclusive jet cross section, which extends the measurement to the forward rapidity region of $|\eta| < 3$, in five rapidity bins. All the measurements show good agreement with the NLO QCD predictions currently available, as can be seen in figure 2.

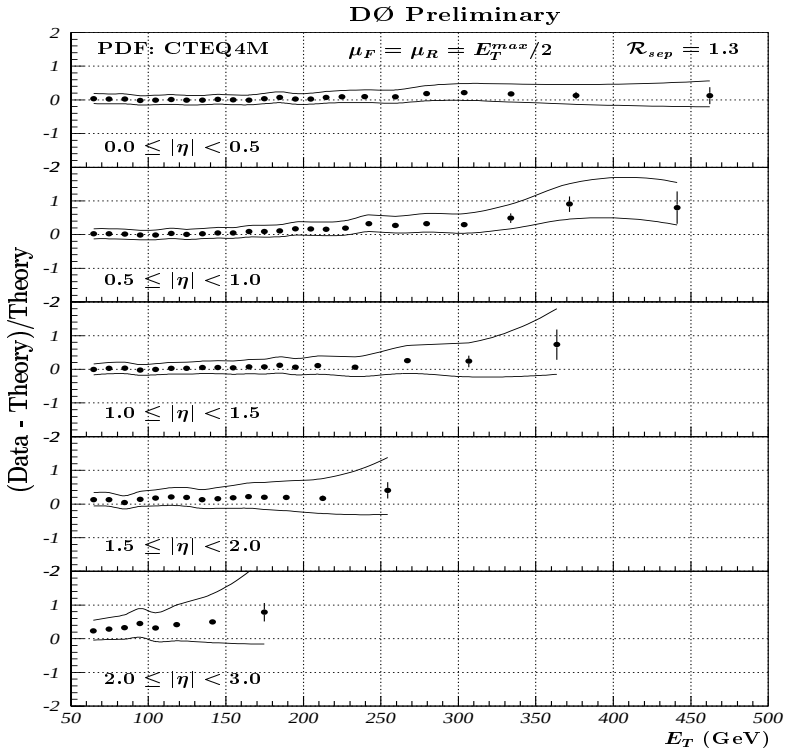

Figure 2: Comparison between the DØ inclusive jet cross section in five pseudorapidity regions (up to $|\eta| = 3.0$) and the α_s^3 QCD prediction with CTEQ4M pdf and the input parameters $\mu_R = \mu_F = E_T^{max}/2$ and $R_{sep} = 1.3$.

Although the Tevatron nominally operated at a center of mass energy of 1.8 TeV, a short period of the time was devoted to collect data at the lower center of mass energy of $\sqrt{s} = 630$ GeV. DØ and CDF measure the ratio of scale invariant cross section $\sigma_S = (E_T^3/2\pi)(d^2\sigma/dE_T d\eta)$ at two center of mass energies as a function of Jet $x_T = E_T/(\frac{\sqrt{s}}{2})$. Figure 3 shows the preliminary results for DØ and CDF. NLO QCD overestimates the DØ data by almost three standard deviations in the medium range of x_T. The disagreement between data and theory is even worse for the CDF data at low x_T. A good quantitative agreement between DØ data and NLO QCD can be obtained if different renormalization scales are used in the theoretical calculation at the two different center–of–mass energies. For instance, a scale of $\mu = 2E_T$ at

$\sqrt{s} = 630$ GeV and of $\mu = E_T/2$ at $\sqrt{s} = 1800$ GeV reproduces the DØ data best. An alternative explanation of the observed discrepancy between CDF data and NLO QCD has been suggested in terms of power–like corrections [9].

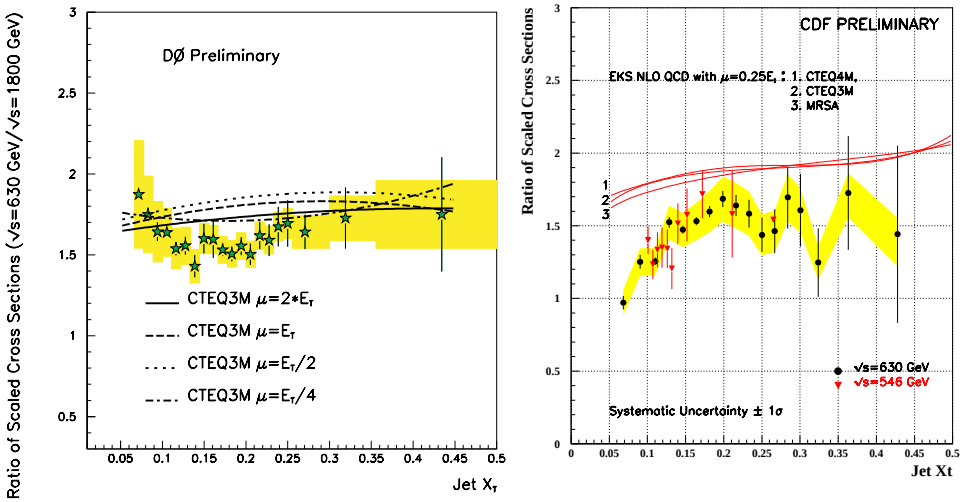

Figure 3: Scale invariant cross section from DØ (left) and CDF (right). Data points are shown with statistical uncertainty; systematic uncertainty is shown as a band. The NLO QCD theoretical predictions for different renormalization scales (left) and different choices of pdf's (right) are shown as lines.

2.2 Dijet Cross Section at Large Rapidity Intervals

Jet production in the high-energy limit of Quantum Chromodynamics (QCD), as defined by center-of-mass energies ($\sqrt{s}$) much larger than the momentum transfers (Q), presents a very interesting and yet little explored area. In this kinematic region, the significantly different energy scales of the process lead to calculated jet cross sections characterized by the appearance of large logarithms $\ln(s/Q^2)$, which must be summed to all orders in α_s. This summation is accomplished through the Balitsky-Fadin-Kuraev-Lipatov (BFKL) [10] equation, which involves a space-like chain of an infinite number of gluon emissions. The gluons have similar transverse momenta, but they are strongly ordered in their pseudorapidities or, equivalently, in their longitudinal momentum fractions, x_i. Thus, the BFKL equation effectively describes the evolution in x (growth with $1/x$) of the gluon momentum distribution in the proton.

Inclusive dijet production at large pseudorapidity intervals ($\Delta\eta$) between the two jets has been suggested as a regime for observing BFKL dynamics. DØ

has measured [11] the dijet cross section for large $\Delta\eta$ in $\overline{p}p$ collisions at $\sqrt{s} = 1800$ and 630 GeV. The result is shown in figure 4. The partonic cross section increases strongly with the size of $\Delta\eta$. The observed growth is even stronger than expected on the basis of BFKL resummation in the leading logarithmic approximation and can be accommodated with an effective BFKL intercept of $\alpha_{\rm BFKL}(20\,{\rm GeV}) = 1.65 \pm 0.07$. It is interesting to note that HERWIG [12] exhibits the same qualitative behavior as the data in that the ratio of cross sections decreases as the $\Delta\eta$ requirement is relaxed, whereas the exact LO calculation predicts a very different trend. A BFKL prediction is not shown for the case of $\Delta\eta > 1$ since the rapidity interval is not sufficiently large for the formalism to be meaningful.

2.3 Subjet Multiplicity in Quark and Gluon Jets

DØ measures the subjet multiplicity in jets reconstructed using the k_T algorithm. Jets with $55 < E_T < 100$ GeV and $|\eta| < 0.5$ are selected from data taken at two center–of–mass energies, $\sqrt{s} = 1800$ GeV and $\sqrt{s} = 630$ GeV.

The HERWIG [12] Monte Carlo event generator predicts that 59% of the jets are gluon jets at $\sqrt{s} = 1800$ GeV, and 33% of the jets are gluon jets at $\sqrt{s} = 630$ GeV. This information is used as input to the analysis to extract the average subjet multiplicity in gluon ($< N_G >$) and quark ($< N_Q >$) jets. DØ clearly distinguishes, on a statistical bases, between quark and gluon jets, as can be seen in figure 4. The measured value of $R \equiv (< N_G > -1)/(< N_Q > -1) = 1.91 \pm 0.04({\rm stat})^{+0.23}_{-0.19}({\rm syst})$ agrees with the Monte Carlo prediction of $R = 1.86 \pm 0.08({\rm stat})$.

3 Boson Production

W and Z bosons, the carriers of the weak force, are directly produced in high energy $p\overline{p}$ collisions at the Fermilab Tevatron. In addition to probing electroweak physics, the study of the production of W and Z bosons provides an avenue to explore QCD, the theory of strong interactions. Direct production of photons is also a powerful tool for testing QCD predictions with fewer of the ambiguities associated with jet production and fragmentation.

3.1 W and Z Production and Decay

CDF and DØ measure the differential $d\sigma/dp_T$ distribution for Z bosons decaying to electrons. The data agrees with the combined QCD perturbative and resummation calculations [13], as can be seen in figure 5. In addition, the DØ $d\sigma/dp_T$ distribution

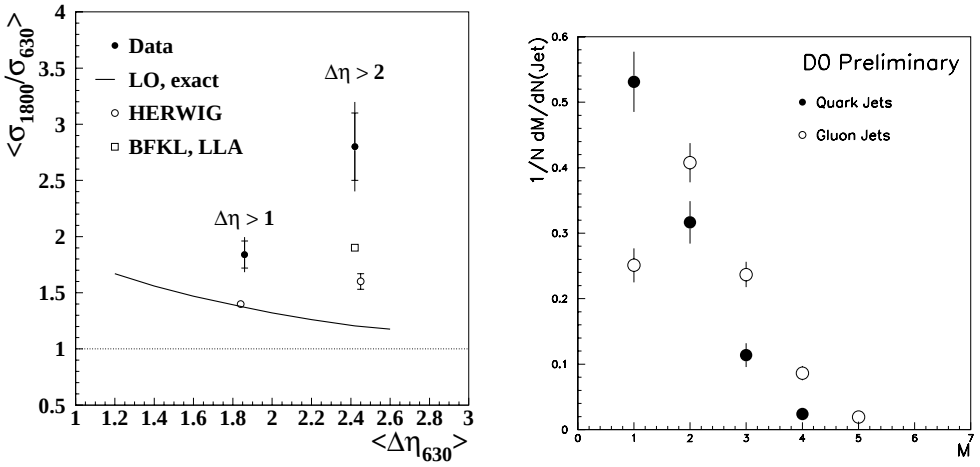

Figure 4: Left: The ratio of the dijet cross sections at $\sqrt{s} = 1800$ and 630 GeV for $\Delta\eta > 1$ and $\Delta\eta > 2$. The minimum jet E_T is 20 GeV. The inner error bars on the data points represent statistical uncertainties; the outer bars represent statistical and uncorrelated systematic uncertainties added in quadrature. The error bars on the HERWIG predictions represent statistical uncertainties. The LO and BFKL predictions are analytical calculations. Right: Subjet multiplicity for quark and gluon jets as measured by DØ.

for the Z boson discriminates between different vector boson production models and can be used to extract values of the non-perturbative parameters for the resummed prediction from a fit to the differential cross section. Figure 6 compares DØ Z data to the fixed-order perturbative QCD theory [14] in terms of a percentage difference from the prediction. We observe a strong disagreement at low-p_T, as expected due to the divergence of the NLO calculation at $p_T = 0$, and a significant enhancement of the cross section relative to the prediction at moderate values of p_T, confirming the enhancement of the cross section from soft gluon emission.

DØ measures the electron angular distribution parameter α_2 in $W \to e\nu$ decays. This measurement is of importance, because it provides a test of next-to-leading order QCD corrections which are a non-negligible contribution to the W mass measurement. The results are compared with next-to-leading order perturbative QCD, which predicts an angular distribution of $(1 \pm \alpha_1 \cos\theta^* + \alpha_2 \cos^2\theta^*)$ [15], where θ^* is the polar angle in the Collins-Soper frame [16]. In the presence of QCD corrections, the parameters α_1 and α_2 become functions of p_T^W, the W boson transverse momentum. DØ presented the first measurement of α_2 as a function of p_T^W, which is shown in figure 7. The QCD prediction is preferred by $\approx 2.3\sigma$ over a $(V - A)$ theory without QCD effects taken into account.

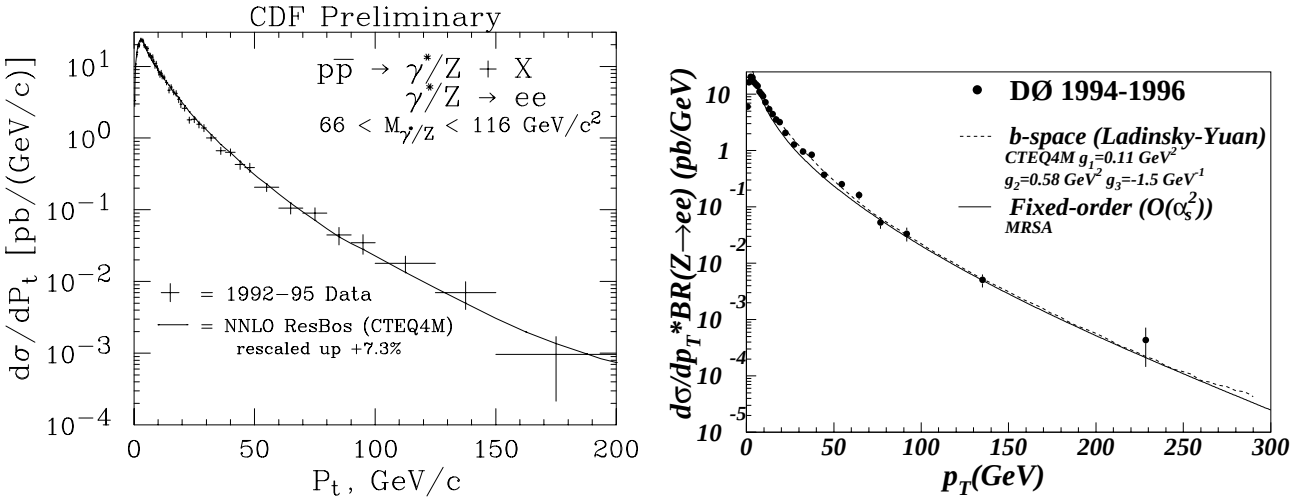

Figure 5: The Z boson transverse momentum spectrum from CDF (left) and DØ (right).

3.2 Photon Production

DØ presented a new measurement [17] of the cross section for the production of isolated photons, with transverse energies E_T above 10 GeV and pseudorapidities $|\eta| < 2.5$. The results are based on a data sample of 107.6 pb^{-1} recorded during 1992–1995. Figure 8 shows that the measured cross section is in good agreement with the next–to–leading order (NLO) QCD calculation [18] for $E_T > 36$ GeV.

CDF measures the inclusive photon cross section in the central region $|\eta| < 0.9$ using 87 pb^{-1} taken during the 1994–1995 $p\overline{p}$ collider run. Figure 8 shows the data compared to variations of the model by Vogelsang *et al.* [19], in which the renormalization, fragmentation and factorization scales are changed independently. None of these changes allows the theory to agree with the data over the entire E_T region.

E706 uses data accumulated from a proton beam at 800 GeV/c on Be target and measures the π^0 and direct–photon inclusive cross section as functions of p_T. The measurements are shown in figure 9 compared to NLO QCD with and without k_T enhancement [20]. Current pQCD calculations fail to account for the measured cross sections using conventional choices of scales. A simple implementation of supplemental parton k_T in pQCD calculations [21], with $< k_T > \sim 1$, provides a reasonable description of the data. E706 obtained similar results using a proton beam at 530 GeV/c, and a π^- beam at 515 GeV/c, and using a hydrogen target.

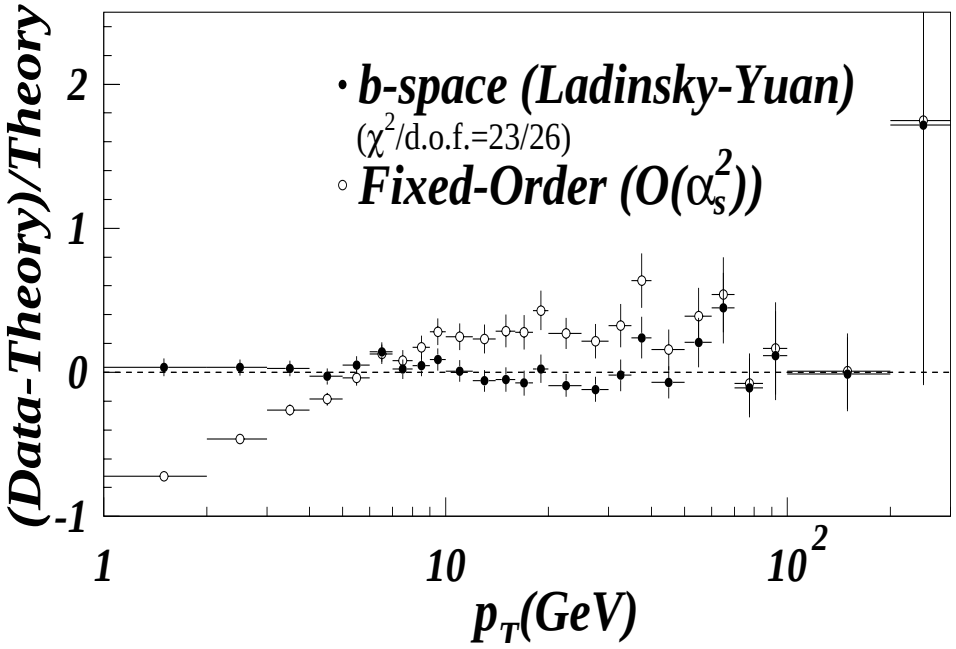

Figure 6: A comparison of data to the resummed and fixed-order ($\mathcal{O}(\alpha_s^2)$) calculations. Also shown are the fractional differences in absolute cross sections between data and the resummed and fixed-order calculations. The uncertainties include both statistical and systematic contributions (other than an overall normalization uncertainty from uncertainty in the luminosity).

4 Conclusions

Although the Tevatron experiments have stopped taking data several years ago, the number of new results is overwhelming. The unprecedented precision in the experimental results that is being achieved is confronting theory with experiments at new limits. So far, QCD has held up to all the quantitative tests that were performed. We expect to see improvements in the calculations in the following years while the experiments prepare for a new period of data taking in which the Tevatron will continue to improve our understanding of nature.

5 Acknowledgements

I would like to thank my Tevatron colleagues who have provided me with the results included in this writeup. I would also like to thank the La Thuile 2000 organizers

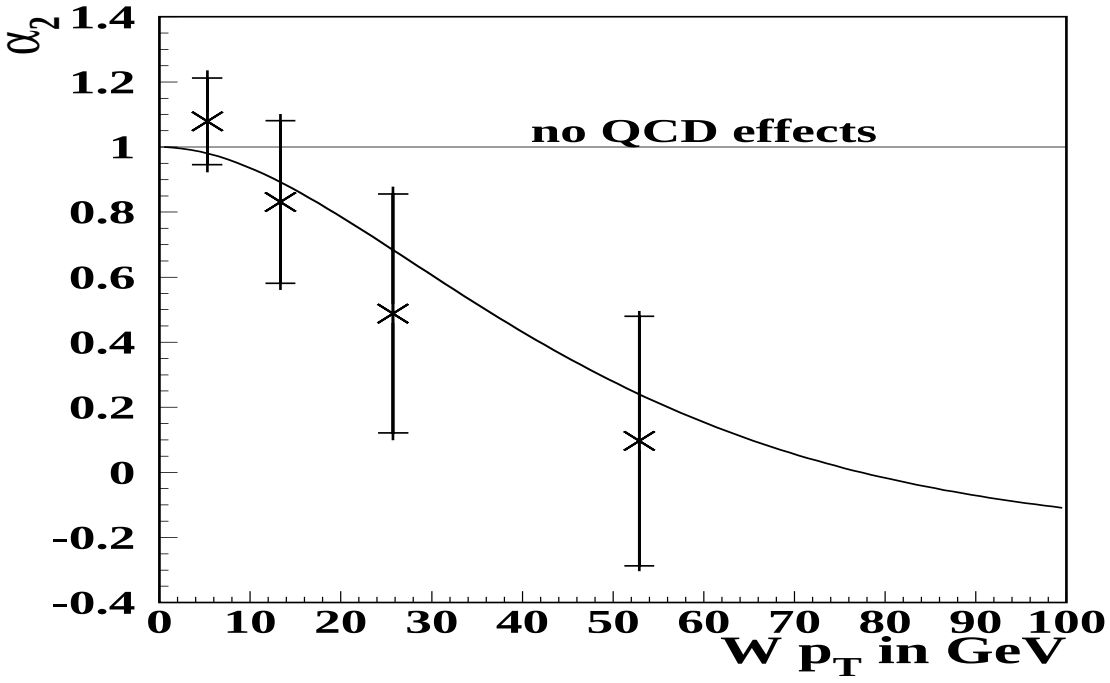

Figure 7: Measured α_2 as a function of $p_T$compared to NLO QCD calculation by Mirkes (curve) and calculation in the absence of QCD (horizontal line). The vertical bars denote the total errors while the statistical errors are marked by horizontal ticks.

for an extremely interesting workshop.

References

1. S. D. Ellis, Z. Kunszt, and D. E. Soper, Phys. Rev. Lett.**64**, 2121 (1990).

2. F. Aversa, *et al.* , Phys. Rev. Lett.**65**, (1990).

3. W. T. Giele, E. W. N. Glover, and D. A. Kosower, Phys. Rev. Lett.**73**, 2019 (1994).

4. H. L. Lai *et al.*Phys. Rev. D55128097.

5. A. D. Martin *et al.*, Eur. Phys. J. **C4**, 463 (1998).

6. The DØ Collaboration, Phys. Rev. Lett. **82** 2451 (1999)

7. W.T. Giele, E.W.N. Glover and D.A. Kosower, Phys. Rev. Lett. **73**, 2019 (1994).

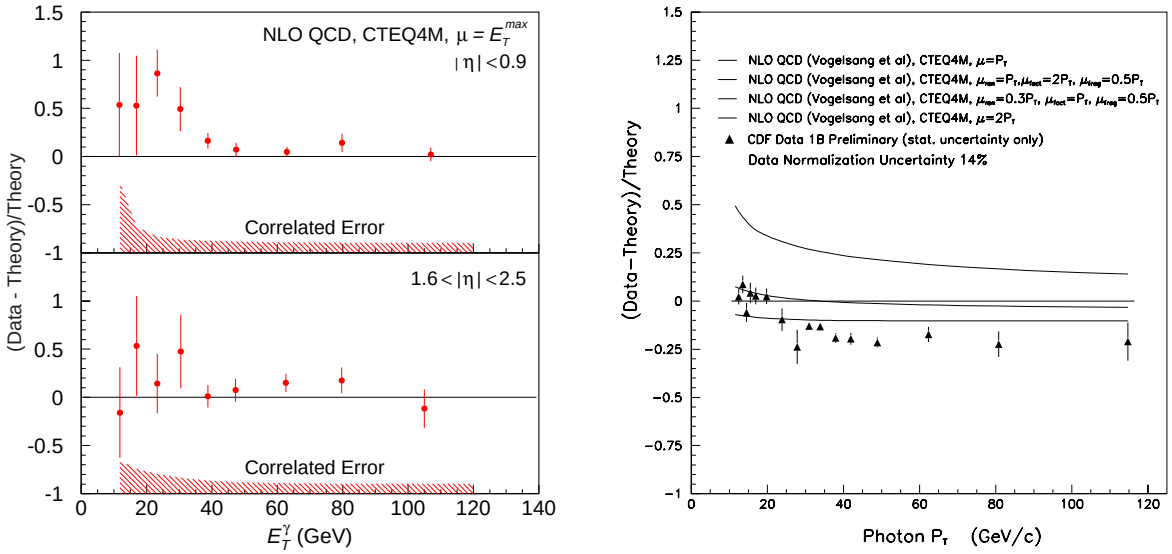

Figure 8: Left: Difference between the measured differetial cross section for isolated photons from DØ and the prediction from NLO QCD, using CTEQ4M parton distributions. Right: Comparison of the CDF inclusive photon cross section with the latest QCD predictions [20] shown using a wide range of scale choices.

8. The DØ Collaboration, Phys. Rev. Lett. **82** 2457 (1999)

9. M. Mangano, hep–ph/9911256

10. L.N. Lipatov, Sov. J. Nucl. Phys. **23**, 338 (1976);
    E.A. Kuraev, L.N. Lipatov, and V.S. Fadin, Sov. Phys. JETP 44 (1976) 443; Sov. Phys. JETP **45**, 199 (1977);
    Y.Y. Balitsky and L.N. Lipatov, Sov. J. Nucl. Phys. **28**, 822 (1978).

11. The DØ Collaboration, Accepted by Phys. Rev. Lett. hep-ex/9912032.

12. G. Marchesini *et al.*, Comput. Phys. Commun. **67**, 465 (1992).

13. C. Balasz and C. P. Yuan, Phys. Rev. D **56**, 5558 (1997).

14. P. B. Arnold and M. H. Reno, Nucl. Phys. **B319**, 37 (1989).

15. E. Mirkes. Nuclear Physics, **B387**, 3 (1992)

16. J.C. Collins, D.E. Soper. Phys. Rev. D **16**, 2219 (1977)

17. The DØ Collaboration, Phys. Rev. Lett. **84** 2786 (2000).

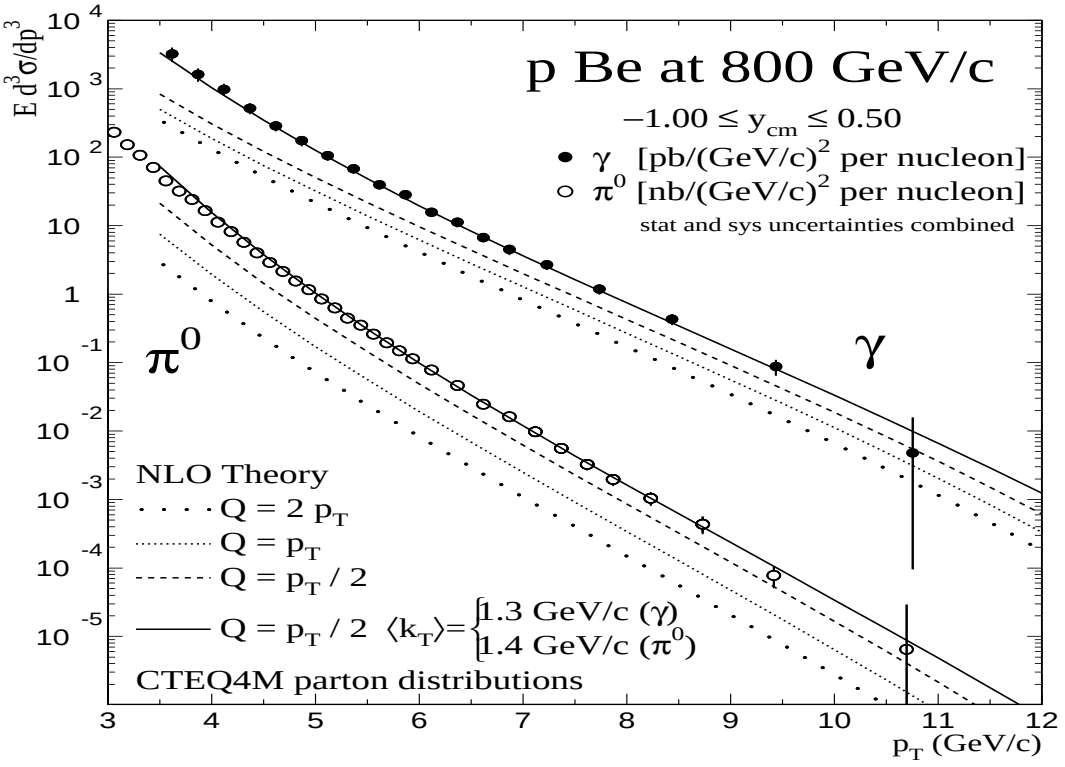

Figure 9: Invariant cross sections for direct–γ and π^0 production from E706. Curves represent the NLO pQCD prediction with and without supplemental parton k_T smearing.

18. H. Baer *et al.*, Phys. Rev. D **42**, 61 (1990).

19. W. Vogelsang and A. Vogt, Nucl. Phys. **B** 453, 334 (1995).

20. E706 Collaboration, L. Apanasevich *et al.*, Phys. Rev. Lett. **81**, 2642 (1998).

21. L. Apanasevich *et al.*, Phys. Rev. D **59**, 074007 (1999).